OPTIMUM DESIGN OF CORRUGATED WIDE COLUMNS

M. H. Magie
C. H. Steinberg

SEPTEMBER 1965
REPORT NO. 65-37

Report No. 65-37
September 1965

OPTIMUM DESIGN OF CORRUGATED WIDE COLUMNS

M. H. Magie
C. H. Steinberg

Department of Engineering
University of California
Los Angeles, California

FOREWORD

The research described in this report, "Optimum Design of Corrugated Wide Columns, "No. 65-37, by M. H. Magie and C. H. Steinberg, was carried out under the direction of F. R. Shanley, Principal Investigator, in the Department of Engineering, University of California, Los Angeles.

This project was conducted under the sponsorship of the National Aeronautics and Space Administration.

Submitted in partial fulfillment of
Contract Number NsG-423.

TABLE OF CONTENTS

INTRODUCTION

A wide column is an axial-compression member which has a width considerably greater than the thickness and for which the unloaded edges are free. The load is applied as a distributed force. The loaded edge is assumed to be simply supported; for other end conditions the effective pin-ended length, L_e, will be used. Reference 1 shows that the trapezoidal corrugation is an efficient type of structure for many types of force transmission. This report deals only with the optimum design of wide columns made of trapezoidal corrugations. Optimization is interpreted to mean the achievement of a minimum weight structure for a specified strength.

Such a design is achieved by arranging the cross section so that the two governing modes of failure occur at the same load. In the case of the wide column the two modes of failure considered are the Euler-Engesser, or general buckling of the column, and the local buckling of the panel element. Figure 1 shows the variation of the two buckling stresses as the panel width is varied. The maximum stress for the given length and area obviously occurs when the two buckling modes occur simultaneously.

Since this type of structure is transmitting a distributed force, it is convenient to use parameters that are related to a unit width. This allows the results to be applied to a column of any width. To eliminate the magnitude of loading and the length as independent parameters the structural index is used. This index is a measure of the loading intensity; it should therefore have the dimensions of a stress. In the case of the wide column the structural index is the load per unit width, q, divided by the length, q/L_e, or P/BL_e where B is the total width.

The cross section of minimum weight was derived by maximizing the axial stress. The optimum cross section was found to be a 60^o trapezoidal corrugation. A comparison was made between the buckling load of the 60^o corrugation and that of the 90^o square corrugation. The theory predicts that the optimum stress for the 60^o corrugations will be fourteen percent greater

than the optimum stress for the 90^{o} corrugations, at a given structural index. The theoretical predictions were supplemented by a test program. Tests were also run on 60^{o} corrugations to demonstrate the validity of the theory.

A practical consideration in the design of wide columns is that of minimum or standard commercially available sheet thicknesses. It is necessary to know what the weight penalty will be for using standard sheet thicknesses. An analysis of this problem was made by Harrington (Reference 2) and is shown in Appendix A.

SYMBOLS

A	=	area of column, in.^{2}
B	=	width of column, in.
b	=	width of corrugation panel, in.
E	=	modulus of elasticity, psi (lb/in.^{2})
E_t	=	tangent of modulus, psi
I	=	moment of inertia, in.^{4}
K_c	=	constant in local buckling equation = 3.60 for simply supported panel
L_e	=	effective length of column, in.
P	=	applied load on column, lb.
q	=	load per unit width, = P/B = lb/in.
t	=	thickness of sheet, in.
$\bar{t}$	=	average thickness, = A/B, in.
w	=	weight per unit width
σ_{cr}	=	Euler-Engesser buckling stress, psi
σ_{cc}	=	local buckling stress, psi
θ	=	angle of corrugations, degree
ρ	=	radius of gyration = $\sqrt{I/A}$, in.
η	=	inelastic factor
η_t	=	tangent modulus ratio, = E_t/E

THEORY

The two modes of failure for the corrugated wide column are the general, or Euler-Engesser, failure described by

$$\sigma_{cr} = \frac{\pi^2 \eta_t E}{(L_e/\rho)^2} \tag{1}$$

(shown in Figure 2)

and the local buckling mode, described approximately by

$$\sigma_{cc} = K_c \eta_t E \left(\frac{t}{b}\right)^2 \tag{2}$$

(shown in Figure 3).

The general buckling stress can be expressed in terms of the structural index, q/L_e, by rearranging terms and noticing that

$$\sigma_{cr} = P/A = \frac{P/B}{A/B} = q/\bar{t} \tag{3}$$

The result is

$$\sigma_{cr}^3 = \left(\frac{\pi^2 \eta_t E}{L_e^2} \rho^2\right) \left(\frac{q^2}{\bar{t}^2}\right)$$

$$\sigma_{cr} = \pi^{2/3} (\eta_t E)^{1/3} \left(\frac{\rho}{\bar{t}}\right)^{2/3} \left(\frac{q}{L_e}\right)^{2/3} \tag{4}$$

To apply this to the corrugation, ρ and $\bar{t}$ must be expressed in terms of b and t. For each corrugation, Figure 4,

$$I = 2\frac{b^3 t}{3} \sin^2\theta \tag{5}$$

$$A = 4bt \tag{6}$$

$$\rho = \sqrt{\frac{I}{A}} = 0.408\, b \sin\theta \tag{7}$$

$$\bar{t} = \frac{A}{B} = \frac{2bt}{b(1+\cos\theta)} = \frac{2t}{(1+\cos\theta)} \tag{8}$$

$$\frac{\rho}{\bar{t}} = \frac{.408\, b \sin\theta}{2t} (1+\cos\theta)$$

$$\frac{\rho}{\bar{t}} = .204 \frac{b}{t} \sin\theta (1+\cos\theta) \tag{9}$$

To obtain an optimum or minimum weight section, the area must be minimized. This can be accomplished by maximizing the stress equation, Eq. (4).

The cross section that will maximize this expression will be the one that has a maximum $\rho/\bar{t}$. This occurs when

$$.204 \frac{b}{t} \sin\theta (1+\cos\theta) = \text{maximum.}$$

Setting the derivative of this expression equal to zero we have

$$\frac{d}{d\theta}\left[\sin\theta (1+\cos\theta)\right] = 0$$

$$(1+\cos\theta)\cos\theta - \sin^2\theta = 0$$

$$\cos\theta = \sin^2 - \cos^2\theta \tag{10}$$

$$\cos\theta = -\cos 2\theta$$

$$\theta_{opt} = 60^{o}$$

Thus, the optimum cross section is achieved when $\theta = 60^{o}$. At this value of θ, Eq. (9) reduces to

$$\frac{\rho}{\bar{t}} = .265 \frac{b}{t} \tag{11}$$

When Eq. (11) is substituted into Eq. (4), the result is

$$\sigma_{cr} = .946 (\eta_t E)^{1/3} (q/L_e)^{2/3} (b/t)^{2/3} \tag{12}$$

Optimization for a given value of the index is obtained by arranging the cross section so that two modes of failure occur simultaneously. To obtain the relationship between the optimum stress and the structural index, substitute from Eq. (2) for b/t and let $\sigma_{cc} = \sigma_{cr} = \sigma$. This gives

$$q/L_e = \frac{0.632\sigma^2}{\eta_t^{3/4} E} \tag{13}$$

or

$$\sigma_{opt.} = 1.26\, \eta_t^{3/8}\, E^{1/2}\, (q/L_e)^{1/2} \tag{14}$$

This is plotted in Figure 5.

For the 90^o corrugation, a similar analysis is performed. Using $\theta = 90^o$ in the equations developed, $\sin\theta = 1$ and $\cos\theta = 0$, the optimum stress is now

$$\sigma_{opt.} = 1.11\, \eta_t^{3/8}\, E^{1/2}\, (q/L_e)^{1/2} \tag{15}$$

The two curves (Equations 14 and 15) are compared on Figure 6.

EXPERIMENTAL PROGRAM

Twenty-six 60^{o} corrugated wide columns were tested to check the validity of the theoretical development. These columns were made from 2024-T3 bare aluminum sheet. All the columns were formed on a leaf brake and the corrugations were oriented along the direction of rolling of the sheet. Table I shows the cross sectional dimensions of the columns.

To provide a uniform distribution of the compressive load the ends of the columns were cast into aluminum channels, using a high strength-low shrinkage plaster, Ultracal 30. The channels were machined to insure that they were flat and parallel. Figure 7 shows a typical test specimen after testing. A fixture was designed that would insure only a pinned support. The freedom of rotation was accomplished by placing a cylindrically machined section of steel on the top of the fixture. The center of rotation of the cylindrical head is at the end of the column. Two adjusting screws control the position of the head so that the load can be transmitted concentrically to the column. Screws on the side of the fixture hold the aluminum channels in place. The fixture can be seen in Figure 8.

The columns were tested on a 60,000 pound Baldwin hydraulic testing machine. An Ames dial indicator was used to indicate the lateral deflection of the midpoint of the column. In some tests two dial indicators were used, on both edges of the column, but it was found that only one was needed. The columns were aligned for concentricity by loading to two-thirds of the predicted failure load and noting the direction of the midpoint deflection. The cylindrical head was then adjusted to obtain the minimal deflection. The two-thirds load point was chosen arbitrarily to keep the column elastic while it was being aligned. The test set-up can be seen in Figure 9.

The fabrication and testing methods used on the 90^{o} corrugations were similar to those of the 60^{o} corrugations except for the forming of the sheets. The leaf brake used for the 60^{o} corrugations did not prove to be adequate. There was insufficient clearance to make more than two successive 90^{o} bends on the leaf brake. For this reason a vertical brake was employed.

This brake incorporates a knife-like vertical action to bend the corrugations. The radius of curvature could be varied to allow for a difference in materials and bending angles. The minimum radius of curvature, 1/8", which was used for the 90^{o} corrugations, is considerably larger than the radius of curvature using the leaf brake.

DISCUSSION

The results of the twenty-six tests on the 60^{o} corrugated columns are tabulated in Table II. The comparison with the theory is shown in Figure 5. There is good agreement between the test data and the theory, although some scatter is evident.

Difficulty was encountered in obtaining concentricity. The cylindrical head of the test fixture was difficult to adjust evenly along the width of the column. The local eccentricities that result from this misalignment affect the strength of the columns. The short columns, having high intensity of loading, are affected more than the long ones.

The plaster that held the column into the channel caused another problem during the testing. As the load increased, the shortening of the column caused the plaster to separate from the aluminum. This separation under load caused the column to shake and in one case, column #7A, the separation occurred near the buckling load and it seemed to cause a premature failure.

A total of twelve specimens were used to compare the 60^{o} to 90^{o} corrugations. Two specimens were tested for each geometrical configuration at the various structural indices to obtain reliability in the test results. The average variation from theory for these specimens was five percent, with a range from 14.6% to 0%. The two theoretical curves have an average stress variation in the plastic range of also about 5% (for a given structural index). Thus, it seems evident that the difference between the two theoretical curves cannot be distinguished in actual application using normal testing procedures.

This hypothesis was further verified by considering an eccentricity which is inherent in the test procedure. Timoshenko (Reference 3) suggests a value of the eccentricity ratio $e/L = 0.0025$. This takes into account such factors as eccentric load application, initial curvature, and material imperfections. A value of $e/L = 0.005$ seems to fit the test data well and it is shown plotted on Figure 6.

The 90^{o} columns had a smaller deviation from the theoretical value than the 60^{o} columns. One factor that contributes to this smaller error is the greater stiffness of the 90^{o} columns. The added stiffness makes the columns less sensitive to initial eccentricities.

Due to the fabrication techniques, the radius of curvature of the corners of the 90^{o} corrugations was larger than that of the 60^{o} corrugations. The larger radius of curvature decreased the flat width, b, of the panel elements. The difference between the theoretical and actual flat panel widths can be seen in Figure 10. This decrease in flat panel width increases the local buckling stress of the columns. Most of the 90^{o} columns had a relatively large lateral deflection, indicative of an Euler-Engesser column failure, before the local buckling occurred.

The relationship between weight and the structural index is shown in Figure 12. This relationship was derived in Appendix A. The greater efficiency of the 60^{o} corrugation is clearly shown in this figure.

CONCLUSIONS

1. The theory developed accurately predicts the behavior of corrugated wide columns. The agreement can be seen in Figure 5.

2. The predicted variation in optimum stress between the 60^{o} and 90^{o} corrugated columns was not conclusively demonstrated by experiment, because experimental errors and differences in fabrication caused some scatter.

REFERENCES

1. Shanley, F. R., Weight-Strength Analysis of Aircraft Structures, Dover Publications, New York, 1960.

2. Harrington, N. M., "The Relative Efficiency of Non-Buckling and Post-Buckling Structures," unpublished Master's Thesis, UCLA, 1962.

3. Timoshenko, S. P. and J. M. Gere, Theory of Elastic Stability, McGraw-Hill, pp. 197-200, 1961.

APPENDIX A

EFFECT OF STANDARD SHEET THICKNESS UPON COLUMN WEIGHT
(Based on Reference 2)

It is often the case that the optimum thickness cannot be economically obtained whereas a standard sheet thickness will be readily available. There are also limitations on minimum thickness. Therefore, the weight penalty for using a sheet thickness other than optimum should be determined.

First, the weight of the column has to be expressed in terms of the design parameters. The average stress on the column can be expressed by

$$\sigma = P/A = q/\bar{t} \tag{A1}$$

The weight per unit width is given by

$$w = d\ \bar{t}\ L_e \tag{A2}$$

where d = density.

Substituting for $\bar{t}$ from Eq. (A1) and rearranging gives an equation relating the dimensionally correct weight parameter and the structural index

$$w/L_e^2 = d\ \frac{q/L_e}{\sigma} \tag{A3}$$

In the optimum column both of the instability modes occur at the same stress and the internal stress (σ) is just sufficient for equilibrium with the external load (q).

$$\sigma_{opt} = \sigma_{cr} = \sigma_{cc} = \sigma$$

where

$$\sigma_{cr} = \frac{\pi^2 \eta_t E}{(L_e/\rho)^2} = \frac{\pi^2 \eta_t E\ b^2\ \sin^2\theta}{6\ L_e^2} \tag{1}$$

and

$$\sigma_{cc} = K_c \eta_t^{1/2} E \frac{t^2}{b^2} \qquad (2)$$

The optimum stress can be expressed in terms of the structural index by eliminating b and t from the stress equations. This is accomplished by letting

$$\sigma_{opt}^4 = \sigma_{cc} \sigma_{cr} \sigma^2$$

When the expressions are substituted for the stress and rearranged,

$$\sigma_{opt}^4 = \frac{\pi^2 K_c \eta_t^{3/2} E^2}{24} \left(\frac{q}{L_e}\right)^2 \sin^2\theta \ (1+\cos\theta)^2 \qquad (A4)$$

Substituting this expression for σ into Eq. (A3) gives the weight equation as

$$\frac{w}{L_e^2} = d\left[\frac{24(q/L_e)^2}{\pi^2 K_c \eta_t^{3/2} E^2 \sin^2\theta (1+\cos\theta)^2}\right]^{1/4} \qquad (A5)$$

This is shown plotted in Figure 11.

In the elastic range it is possible to show the greater weight efficiency of the 60^o corrugation by taking the ratio of the weight parameter (as the angle varies) to that of the 60^o corrugation. This relationship becomes

$$\frac{(w/L_e^2)\theta}{(w/L_e^2)_{60^o}} = \left[\frac{\sin\theta(1+\cos\theta)}{1.30}\right]^{1/2} \qquad (A6)$$

This is shown as the minimum weight curve on Figure 12 (after Harrington).

This ratio can be expressed in terms of the ratio of the optimum thickness to the standard thickness by utilizing the relationship

$$\frac{w}{L_e^2} = \frac{d\,\bar{t}}{L_e} \qquad (A7)$$

Thus the ratio becomes

$$\frac{(w/L^2)\theta}{(w/L^2)_{60^o}} = \frac{\bar{t}_s}{\bar{t}_{60^o}} \tag{A8}$$

In terms of the sheet thickness,

$$\frac{(w/L^2)\theta}{(w/L^2)_{60^o}} = \frac{3t_s}{2(1+\sin\theta)\, t_{60^o}} \tag{A9}$$

This expression is shown for various values of t_s/t_{60^o} on Figure 12. The minimum weight point for all these curves lies on the minimum weight curve described by Eq. (A6). For any ratio of available sheet thickness, the angle that will give the minimum weight can be taken from Figure 12.

APPENDIX B

TABLE 1

TEST SPECIMEN DIMENSIONS

60^{o} Flat Corrugations
2024-T3 Aluminum

TEST OF THEORY

Column No.	t in.	b in.	b/t	L in.	L/e
1	0.040	0.060	15	3.05	14.5
2	0.040	0.800	20	5.31	19
3	0.040	0.720	18	4.30	17
4	0.032	0.752	23.5	6.04	23
5	0.032	0.877	27.4	9.07	29.6
6	0.020	0.700	35	14.2	57.9
7	0.020	0.900	45	23.3	73.9
8	0.040	0.800	20	5.31	19
9	0.032	0.875	27.3	9.07	29.6
10	0.020	0.700	35	14.2	57.9

TABLE II

TEST RESULTS

60^{o} Flat Corrugations
2024-T3 Aluminum

Test No.	Col. No.	Predicted Load P_{pred} lb x 10^3	Experimental Load P_{exp} lb x 10^3	% Error	Maximum Stress σ_{max} lb/in^2 x 10^3	Structural Index q/L_e lb/in^2
1	3C	21.9	23.14	5.68	51.3	641
2	3A	21.9	18.94	-13.5	42.0	527
3	3B	21.9	23.02	5.12	51.1	639
4	2C	23.35	23.55	0.86	47.1	475
5	2B	23.35	23.85	2.15	47.7	480
6	2A	23.35	23.6	1.07	47.2	476
7	1B	19.4	16.64	-14.2	44.3	781
8	1C	19.4	17.6	-9.29	46.7	828
9	1A	19.4	18.74	-3.40	49.7	879
10	5A	16.85	16.32	-3.14	37.0	176.5
11	5B	16.85	15.84	-5.95	36.1	172
12	5C	16.85	15.6	-7.41	35.5	169
13	4D	16.2	13.86	-14.4	36.7	263
14	4A	16.2	16.48	1.73	43.6	312
15	4B	16.2	15.58	- 3.84	41.2	294
16	6A	6.48	5.95	-8.20	27.0	51.2
17	6B	6.48	6.16	-4.95	28.0	53.1
18	6C	6.48	6.16	-4.95	28.0	53.1
19	7A	5.38	4.93	- 8.40	17.5	20.2
20	7B	5.38	4.94	-8.20	17.5	20.2
21	7D	5.38	4.84	-10.05	17.2	19.8
22	8A	26.4	28.55	8.14	50.6	531
23	8B	26.4	27.1	2.65	48.0	503
24	9A	19.0	18.0	-5.27	36.4	180
25	9B	19.0	17.0	-10.5	34.4	169
26	10A	7.26	6.98	-3.86	28.1	55.9

TABLE III

TEST SPECIMEN DIMENSIONS-COMPARISON

(1)

90° SQUARE

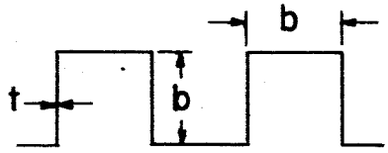

(2)

60° FLAT

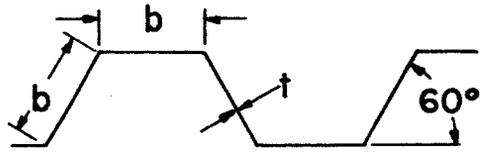

No.	Type	b	t	L	$\rho = f(\alpha, b)$
11a	1	.86	.032	12.6	.359
11b	1	.86	.032	12.6	.359
12a	2	.77	.032	8.13	.266
12b	2	.77	.032	8.13	.266
13a	1	.87	.040	9.76	.371
13b	1	.87	.040	9.76	.371
14a	2	.78	.040	5.91	.275
14b	2	.78	.040	5.91	.275
15a	1	.74	.040	6.08	.302
15b	1	.74	.040	6.08	.302
16a	2	.68	.040	4.19	.241
16b	2	.68	.040	4.19	.241

NOTE: All Values in Inches

TABLE IV

TEST RESULTS - COMPARISON

Type	Theoretical		b/t	L_e/ρ	Experiment		Stress Variation* %	Southwell Diagram e/L x 10^4
	q/L_e psi	$\sigma_{opt.}$ x10^3 psi			q/L_e psi	$\sigma_{opt.}$ x10^3 psi		
11a 90° Sq.	200	36.1	26.7	35.1	194	36.5	0	0.705
11b 90° Sq.	200	36.1	26.7	35.1	192	36.2	-0.55	0.834
12a 60° Flat	200	38.2	24.1	30.0	166	31.7	-14.6	2.03
12b 60° Flat	200	38.2	24.1	30.0	174	33.5	-10.9	1.84
13a 90° Sq.	400	40.5	21.7	26.3	297	38.8	-2.8	1.29
13b 90° Sq.	400	40.5	21.7	26.3	285	37.7	-5.3	2.34
14a 60° Flat	400	44.1	19.4	21.5	402	44.6	1.6	1.86
14b 60° Flat	400	44.1	19.4	21.5	393	42.5	-2.3	2.13
15a 90° Sq.	600	45.4	18.5	20.1	524	44.2	0.68	2.20
15b 90° Sq.	600	45.4	18.5	20.1	561	46.7	4.5	0.891
16a 60° Flat	600	48.1	17.0	17.4	563	44.5	-5.9	2.44
16b 60° Flat	600	48.1	17.0	17.4	537	42.4	-9.2	3.94

*Variation between experimental and theoretical stress at experimental q/L value

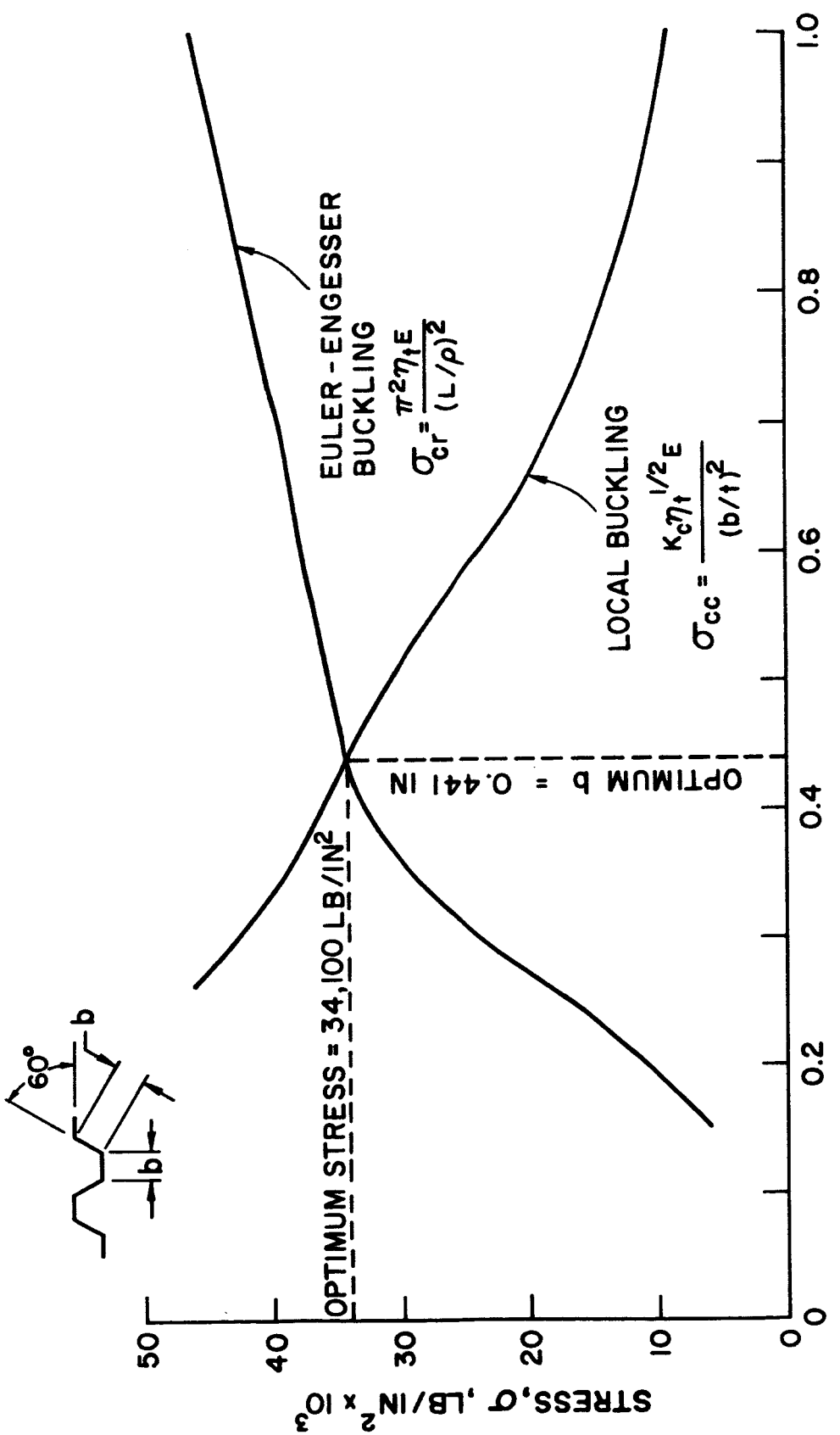

DETERMINATION OF THE OPTIMUM STRESS
Column Length = 7.0 In.
Area Per Unit Width = 0.020 In.
2024 - T3 Aluminum Sheet
60° Corrugation

FIGURE 1

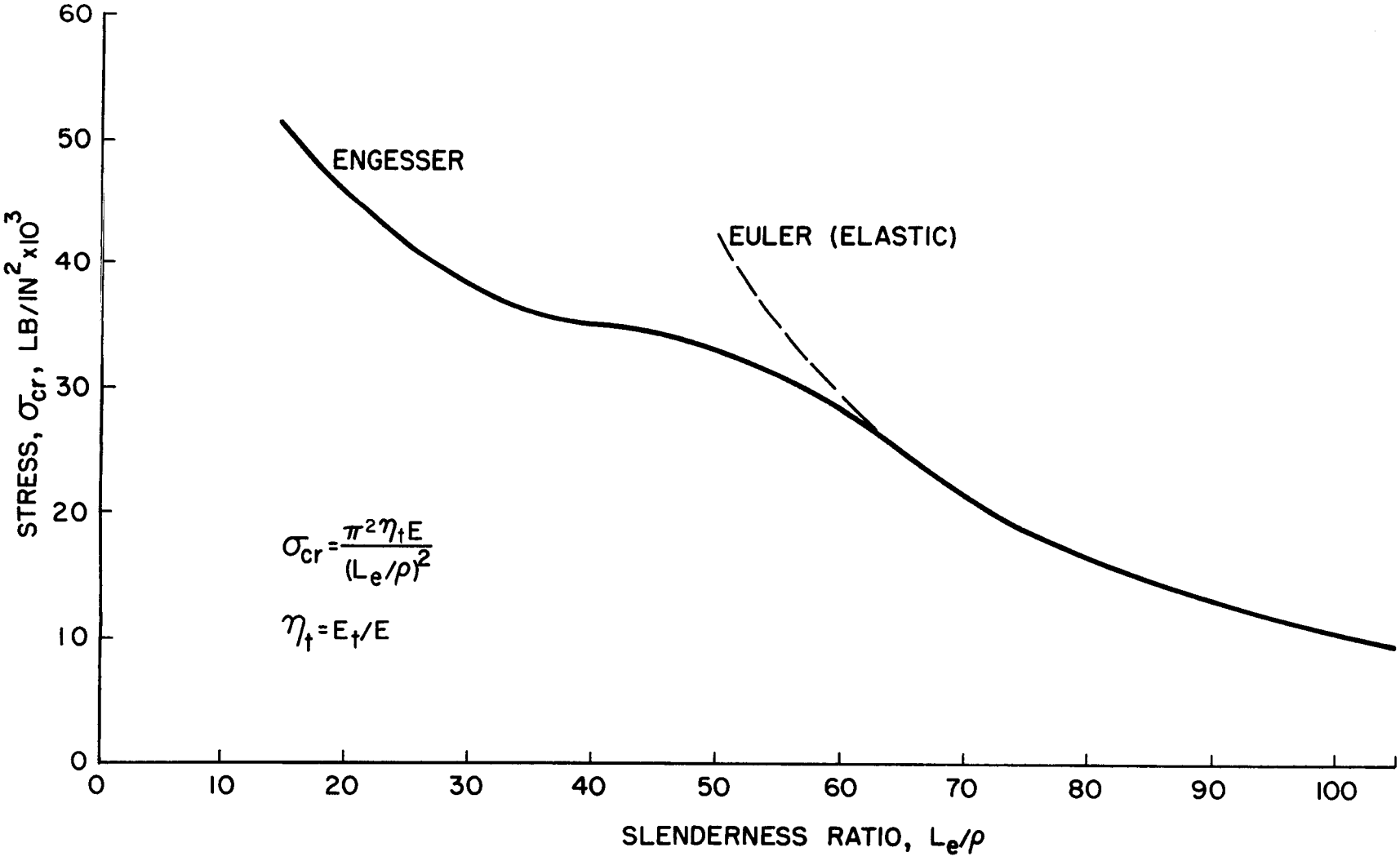

EULER - ENGESSER BUCKLING
2024-T3 Aluminum Sheet

FIGURE 2

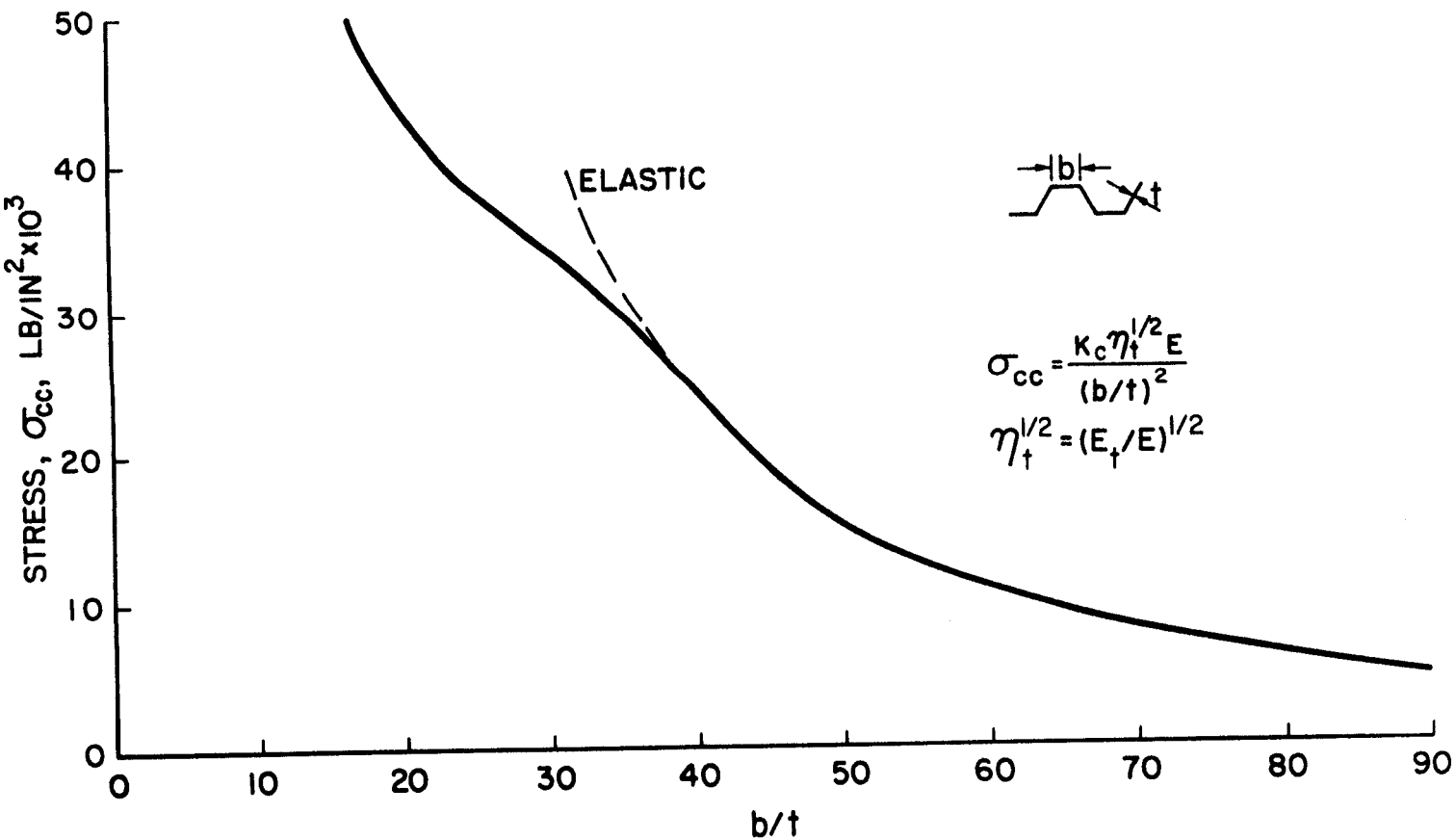

LOCAL BUCKLING
2024-T3 Aluminum Sheet

FIGURE 3

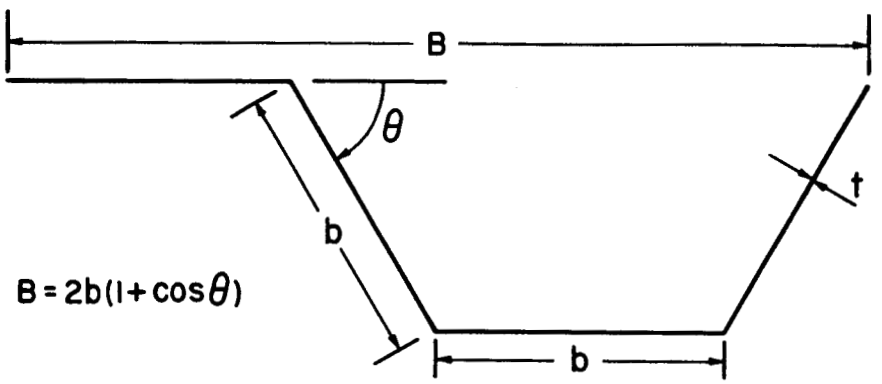

CORRUGATION ELEMENT

FIGURE 4

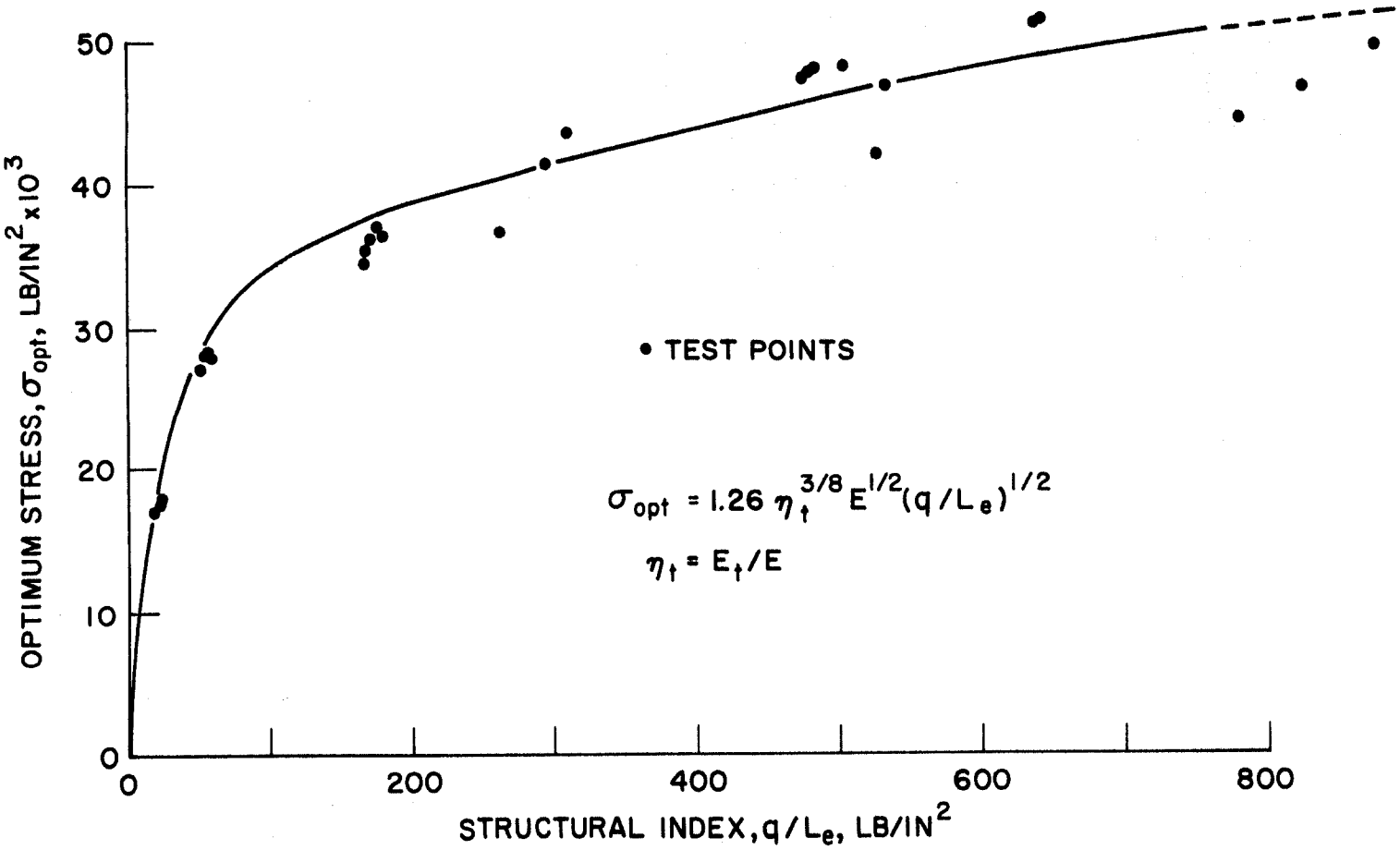

OPTIMUM STRESS VS. STRUCTURAL INDEX
60° Flat Corrugated Wide Columns
2024-T3 Sheet-Longitudinal

FIGURE 5

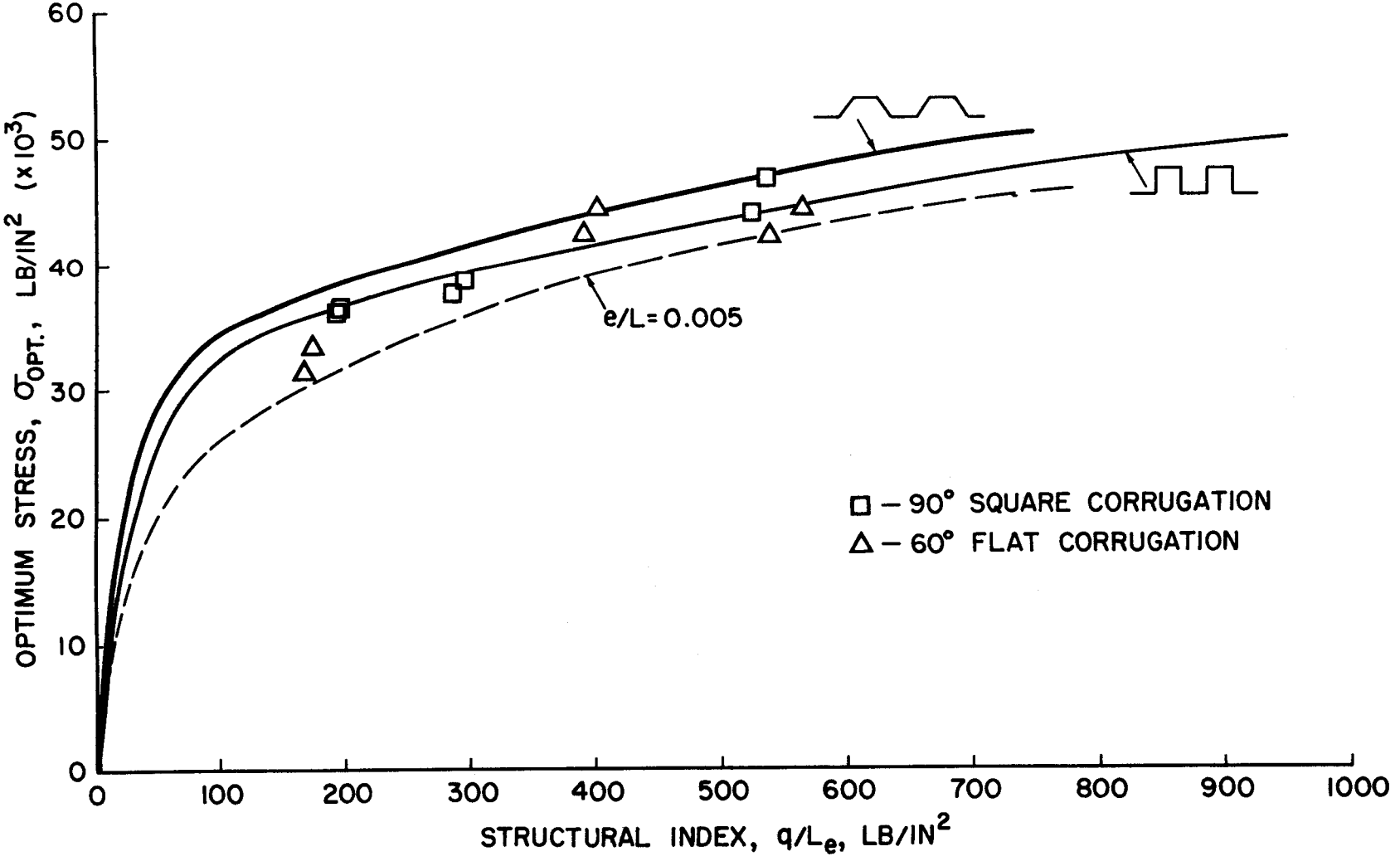

OPTIMUM STRESS VS. STRUCTURAL INDEX FOR
CORRUGATED WIDE COLUMNS IN COMPRESSION
2024-T3 Aluminum Sheet

FIGURE 6

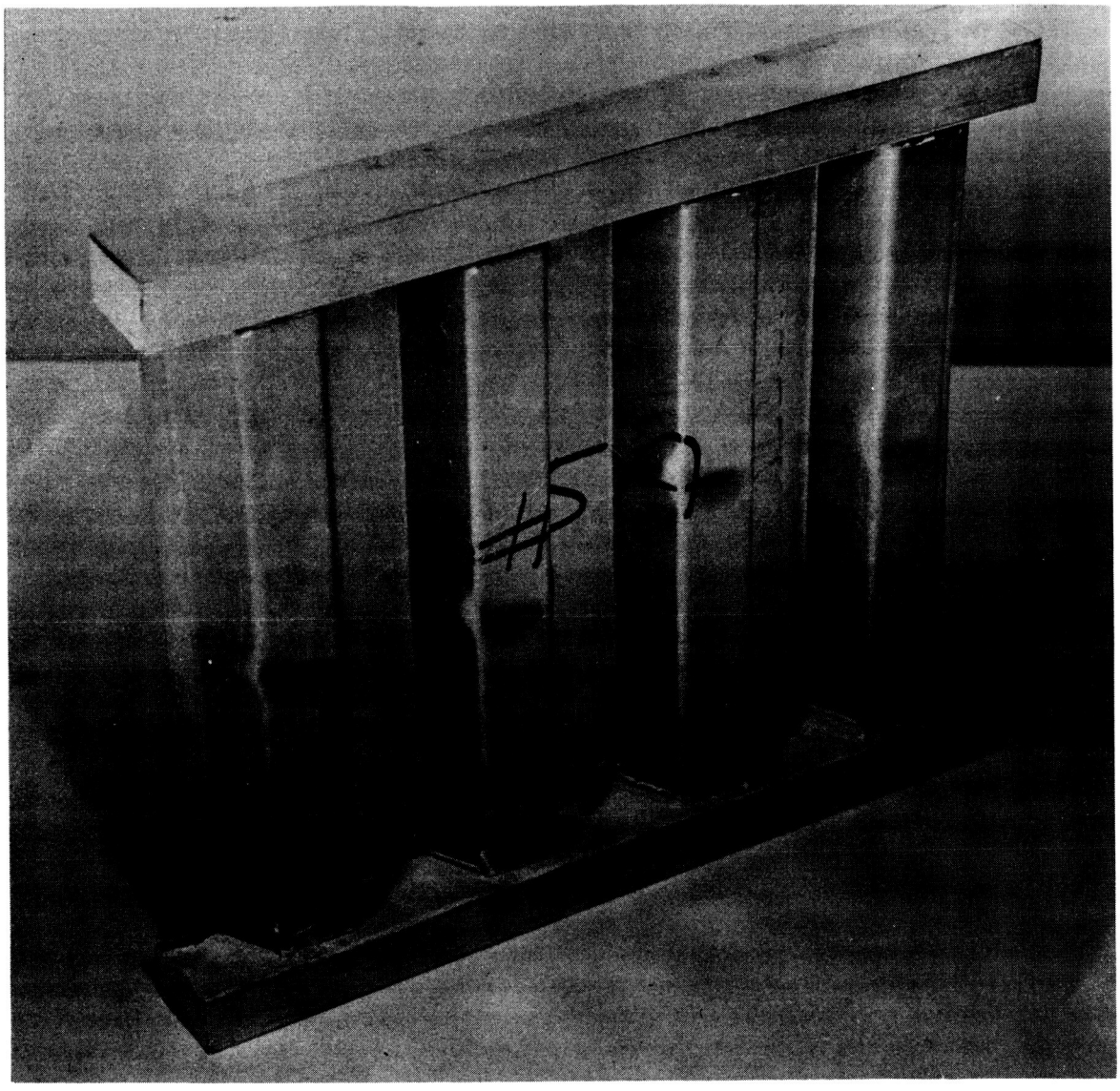

TYPICAL TEST SPECIMEN AFTER TESTING

FIGURE 7

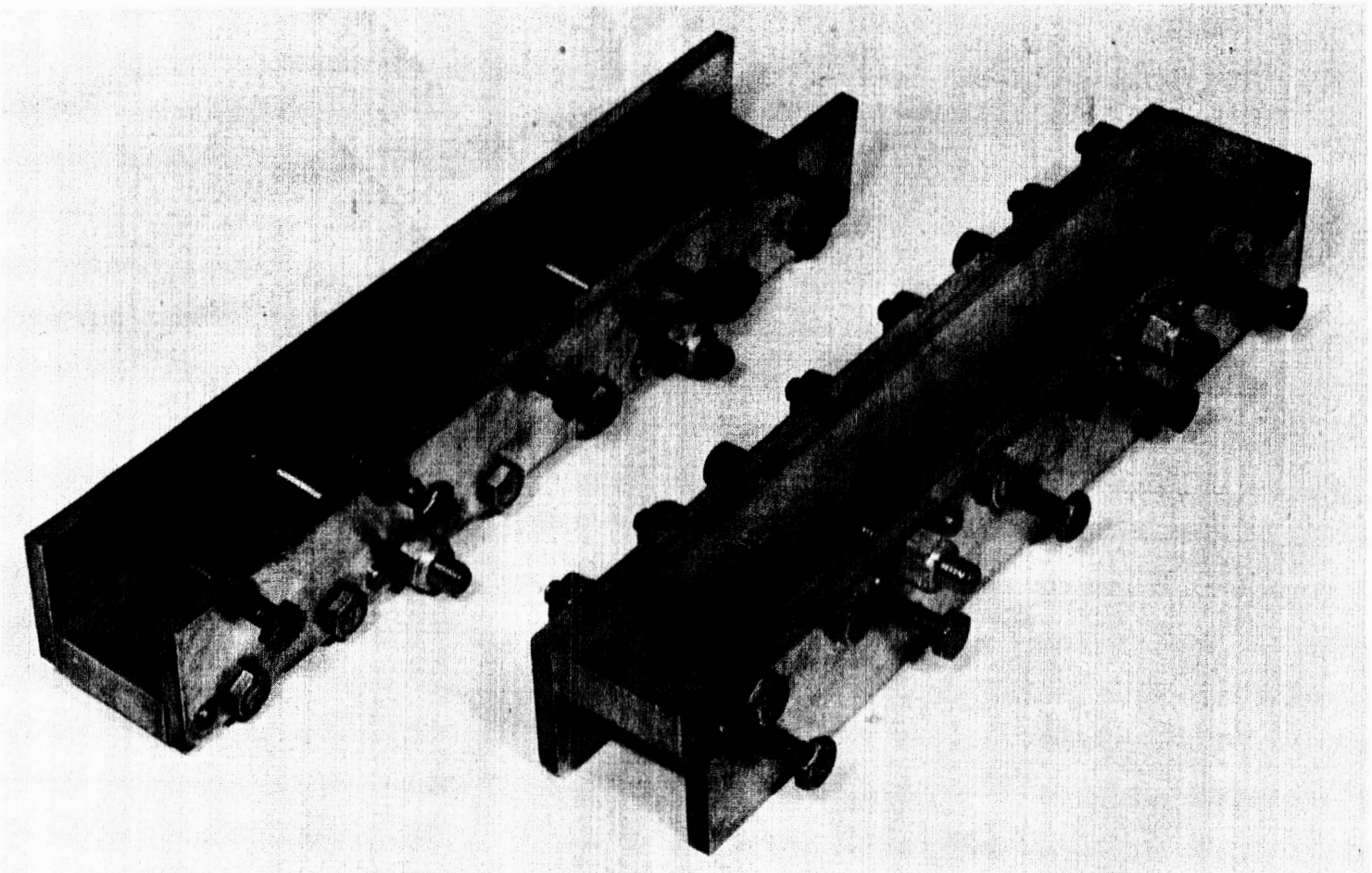

WIDE COLUMN TEST FIXTURE

FIGURE 8

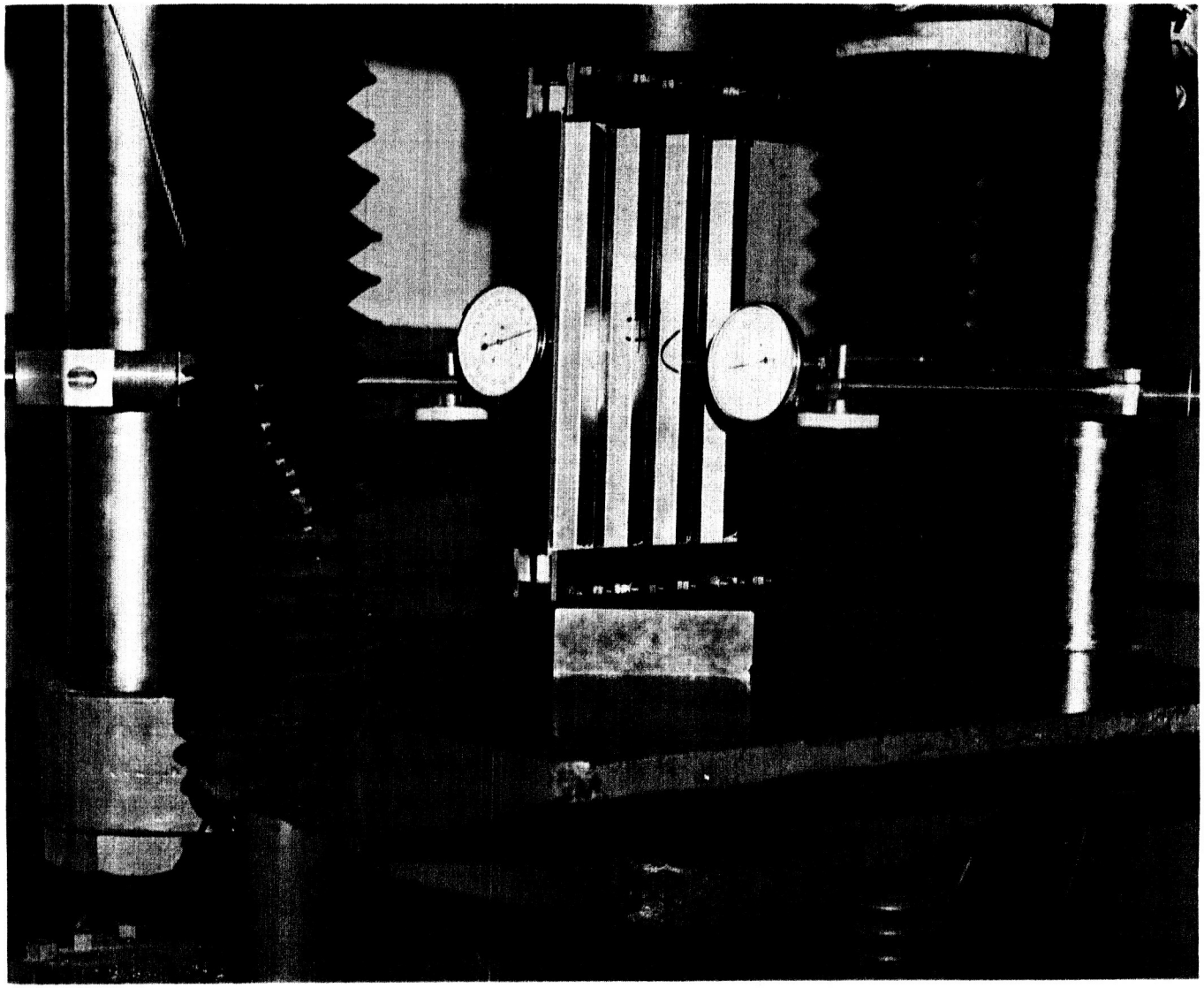

WIDE COLUMN TEST SET-UP

FIGURE 9

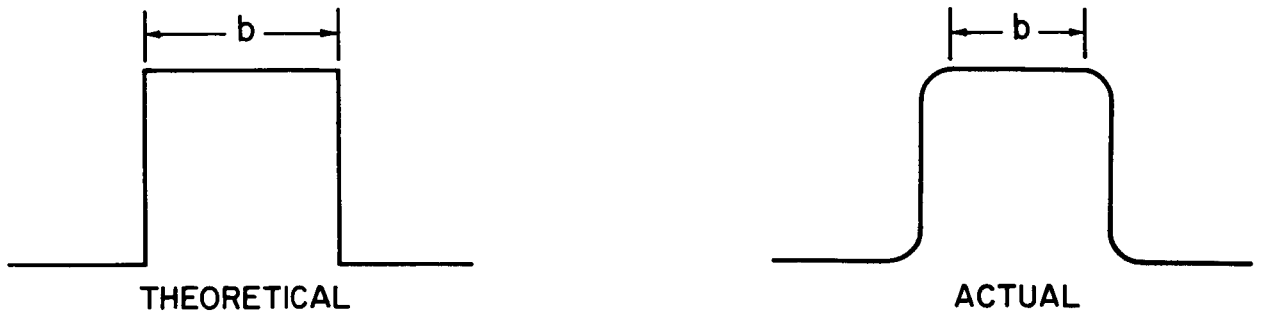

90° CORRUGATIONS

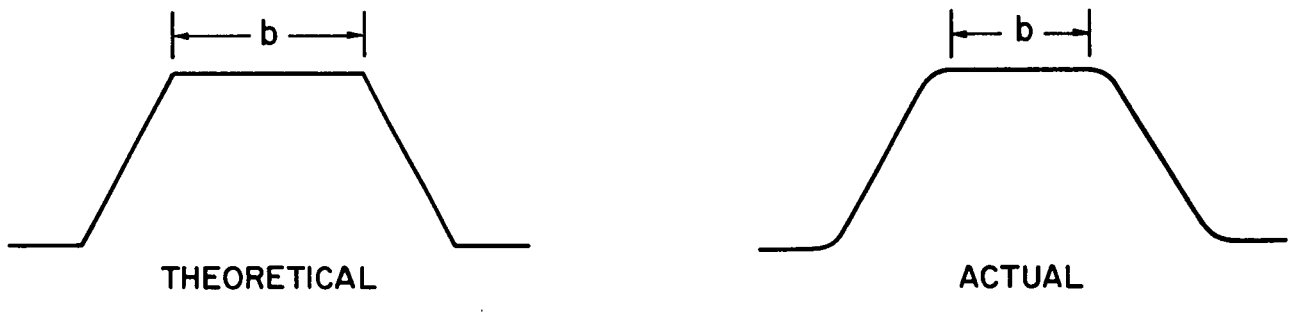

60° CORRUGATIONS

EFFECT OF RADIUS OF CURVATURE ON PANEL WIDTH b

FIGURE 10

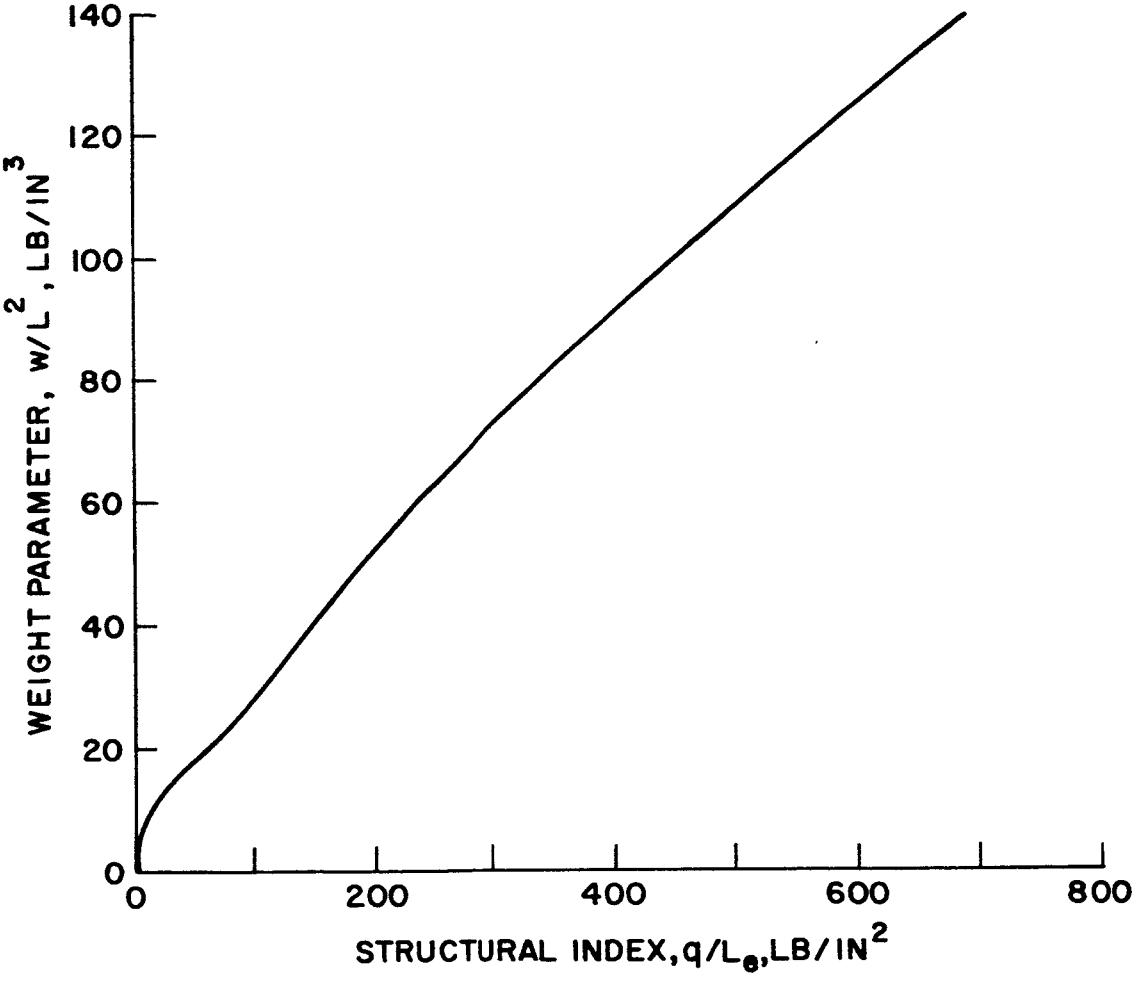

WEIGHT OF OPTIMUM CORRUGATED WIDE COLUMNS
2024-T3 Aluminum Sheet
60^{o} Corrugations

FIGURE 11

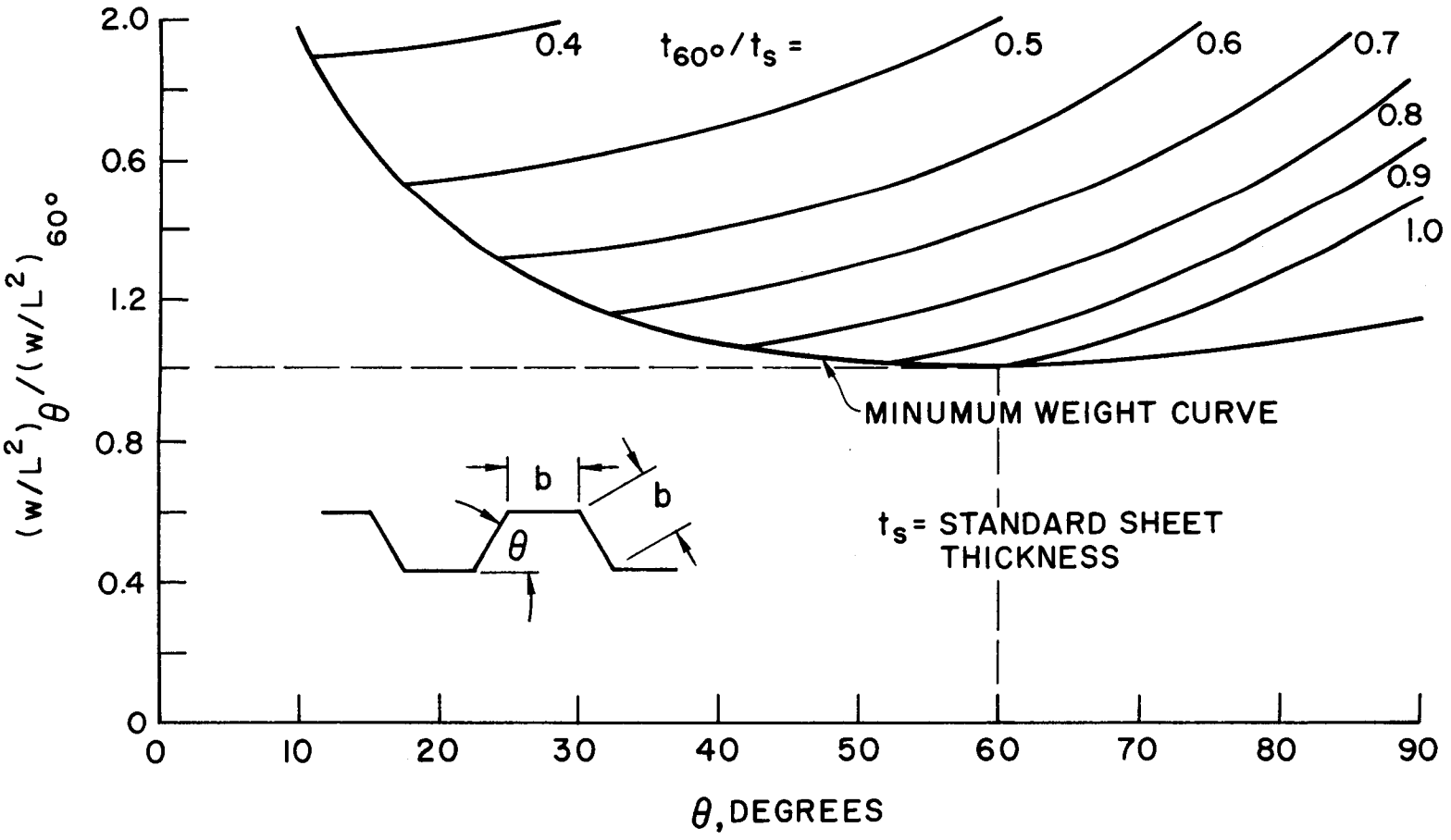

RELATIVE WEIGHTS OF STANDARD SHEET THICKNESS CORRUGATIONS
(Elastic Range)

FIGURE 12